DESENVOLVIMENTO DE REFORÇO DE COMPOSITES DE FIBRA DE CARBONO PARA APLICAÇÃO EM MANGUEIRAS MARÍTIMAS

Maikson L. P. Tonatto[1]*, Maria M. C. Forte[1], Sandro C. Amico[1]

[1]Post-Graduation Program in Mining, Metallurgical and Materials Engineering, Laboratory of Polymeric Materials (LaPol), Federal University of Rio Grande do Sul, P.O. Box 15010, 91501-970 Porto Alegre/RS, Brazil

ABSTRACT

Marine hoses for offshore mooring are commonly used for transferring crude oil and liquid petroleum products, to and from tanker vessels. These hoses are assembled in mooring buoy and FPSO hull. During offloading operations, the hoses are submitted to resist bending radius, collapse and crush loads. GMPHOM 2009 OCIMF Guide specifies some tests as vacuum, minimum bending radius and crush test. The hose inner tube and carcass are examined in these tests. The purpose of the tests is to establish that the hose will be no permanent deformation, such as kinking or ovalling, when returned to the straight position. To fulfill those requirements, typical hose designs carry a metallic steel helix wire in the primary carcass. The steel wire adds approximately 500 kg in weight in an Offloading Hose (20" diameter and 35' length), requiring a thick layer of Expanded Foam in the floating jacket to guarantee the hose buoyancy requirements. In this study, it was carried the structural analysis and calculation of a curved carbon fiber pultruded composite as an alternative material for the steel helix wire. Carbon Fiber Composite Structures are known to be 5 times lower weight than steel and present increased performance in specific mechanical properties. Results in structural analysis, mechanical properties and crush test evaluations are demonstrated.

Keywords: Offloading hose, curved composite structures, progressive damage model, crushing load

1. Introduction

Different systems are used for oil transportation depending on the particular application. In the Early Production System (EPS), the platform can connect directly to the Shuttle Tanker, and in the Catenary Anchor Leg Mooring (CALM), a monobuoy distributes to other hose lines [1]. These may be underwater or floating hoses being bonded flexible pipes. Different types of materials (fibers, steel mesh, rubber, etc.) are subsequently stacked over a mandrel to produce the hose [2].

The main components of the floating hose used in the oil industry are flanges, nipples, rubber layers, reinforcement plies and spirals. The load-bearing component is a wire spiral with crushing and torsional strength. The spiral is usually a solid steel bar, which is applied on the hose following specific diameter, pitch and size [3]. However, steel spirals have high weight and can show plastic strains in some loading cases. Indeed, when subjected to a

bending moment, a crushing load develops on the hose, being considerable for large displacement conditions. This results in tensile load on the upper region and compression load on the lower region. Besides, load intensity decreases from the top or bottom towards the neutral line of the section. These loads are supported by the spiral, which has the function of preventing collapse, obstruction or kinking of the hose. Other common failure mechanism in steel coil is the plastic collapse due to the radial compression load when the bonded hose is subject to high external pressure. Therefore, the development of lightweight structures is considered strategic in this application.

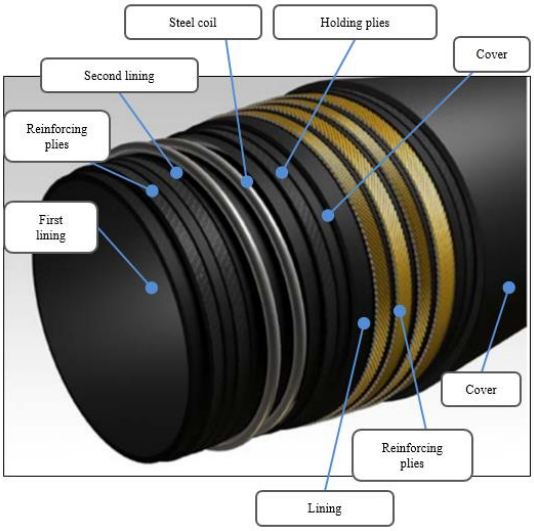

Fig. 1: Photographs of one of the hose sections (a), dimensions [mm] (b) and during the crush test in the Instron machine (c).

The objective of this study is to propose a progressive damage analysis strategy to predict the complex failure behavior of carbon/epoxy composite spirals used as load-bearer in an oil offloading hose. A finite element model is developed based on Multi-continuum Theory (MCT) to determine failure when subjected to radial loading. The potentialities and drawbacks of replacing the steel spiral traditionally used for that by composite spirals are addressed based on numerical and experimental results of crushing.

2. Experimental

A load-bearer composite and steel components were investigated. One spiral shaped samples of circular cross section (diameter 12.7 mm and pitch 36 mm) were manufactured with epoxy resin and carbon fiber (CF) by curved pultrusion (named E/PU/S) as show in Fig. 1. The samples have an average diameter of 560 mm. The curved pultrusion process is a modification of the standard pultrusion process, where the die is no longer stationary, but moves back and forth along the profile. The profile was produced using UTS50 unidirectional carbon fibers oriented to 0º. The fibers were impregnated by an epoxy resin system, and the profile was manufactured using a circular profile die. The cure of the composite material was held right after the profile formation. Afterwards, pieces of 1500 mm length were cut out of the cured material.

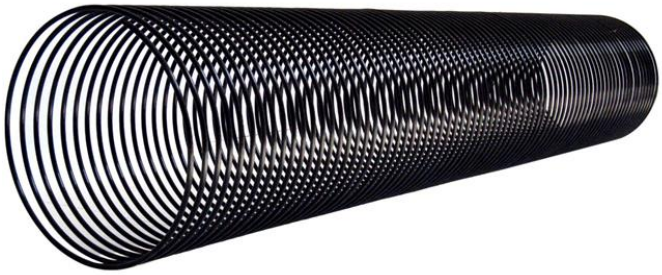

Fig. 2: Photographs of load-bearer composite component manufactured by curved pultrusion - E/PU/S.

Flat regular samples of the same material of the spiral were also produced via the same process than spirals samples were manufactured with longitudinally to the fiber orientation. Axial and transverse extensometers were used for tensile testing at 2 mm/min, according to ASTM D3039. The compressive test was performed at 1.3 mm/min, according to ASTM D6641. The tensile and compression tests were carried Instron 3382 testing machine. The plane shear test was carried out with double V-notched specimens according to ASTM D7078. A strain gage rosette was used and coupled to a data acquisition HBM Spider 8 600 Hz system. Short-beam test was carried out according to ASTM D2344, at 1 mm/min, with curved specimens cut off from spirals samples. Five samples were used in each test. The cross section morphology of the samples was analyzed before and after failure in a Karl Zeiss model Axio Scope A.1 optical microscope.

A single hose, with the various spirals side by side, was manufactured on a 20 in mandrel. The stacking sequence consisted of 14 layers of rubber embedded by a polyester fabric with the same characteristics shown in literature [8]. Then spiral was positioned, and a layer of elastomer was used to fill the gaps in-between them, followed by the deposition of four extra polyester fabric/rubber layers. The assembly was transferred to an autoclave for curing of the elastomer. Later, 500 mm long hose sections (two for each load-bearing component) were cut off and stored for testing Fig. 3(a). All spirals were equally spaced (pitch/distance of 36 mm – Fig. 3b).

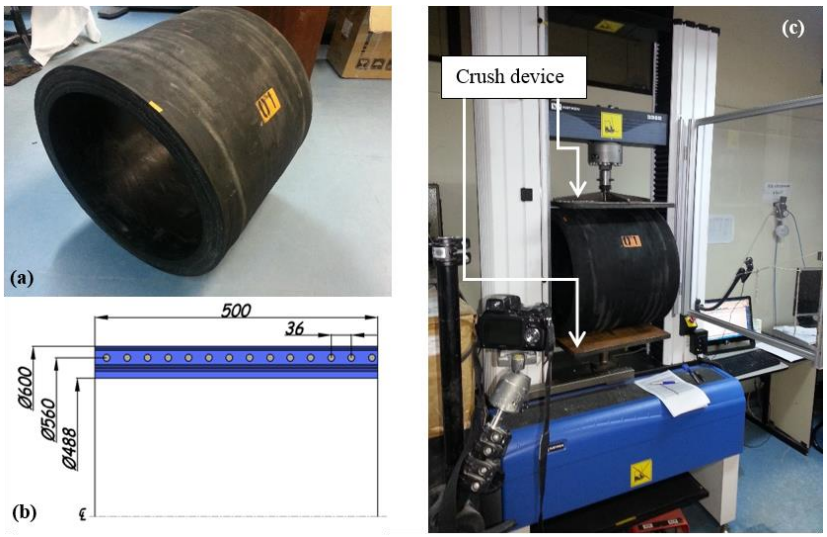

Fig. 3: Photographs of one of the hose sections (a), dimensions [mm] (b) and during the crush test in the Instron machine (c).

A rigid square plate was used to apply compression loading on the top of the sample, leading to crushing, as shown Fig. 3c. A pre-load was applied followed by load increments of equal steps to available the permanent deflection (inelastic deformation). The outer diameter along the plane parallel to the load was measured. The compressive test was performed at 12 mm/min until complete failure of the structure. The permanent (inelastic) and elastic strains were measured. One design criterion for hoses is based on maximum permanent diameter variation of the spiral, which must not exceed 1% when the hose is unloaded [4, 5]. The maximum diameter variation (V) is calculated as:

$$V_1 = \frac{D_{max} - D_o}{D_o} > 1\% \text{ or } V_2 = \frac{D_o - D_{min}}{D_o} > 1\% \quad (1)$$

where D_{max} and D_{min} are the largest and smallest diameters found in any radial direction, D_o is the original manufactured hose diameter in the same radial direction where D_{max} and D_{min} are measured.

3. General Results

Table 1 shows the average values of tensile, compressive and shear properties of the coupons representative of the spiral (E/PU/S). All of them showed satisfactory tensile results. The longitudinal compressive strength was 54% lower than the longitudinal tensile strength. The longitudinal modulus E_{11} was much higher than the transverse modulus E_{22} = E_{33}, as expected. The shear strength τ_{13} showed different values to the interlaminar strength τ_{sb} obtained in the short beam test. The applied loading in short-beam test creates high local stress concentrations, and the short length of the beam does not permit large zones of uniform shear stress. Shear stress state is more complex than the pure shear stress predicted by the simple classical beam theory, which ignores the non-symmetric distribution of the transverse shear stress across the specimen [6, 7].

Table 1: Elastic properties and strength values of the representative coupons.

	Symbol	*E/PU/S*
Elastics constants	ρ_c (g/cm³)	1.49 ± 0.01
	V_f (%)	61.3 ± 0.6
	E_{11} (GPa)	116.3 ± 4.7
	$E_{22} = E_{33}$ (GPa)	7.9
	$\nu_{12} = \nu_{13}$	0.32 ± 0.02
	ν_{23}	0.37
	$G_{12} = G_{13}$ (GPa)	4.05 ± 0.56
	G_{23} (GPa)	2.87
Strengths	σ_{11}^T (MPa)	1878.1 ± 101.2
	σ_{22}^T (MPa)	59.0
	σ_{11}^C (MPa)	937.0 ± 99.0
	σ_{22}^C (MPa)	213.0
	$\tau_{12} = \tau_{13}$ (MPa)	68.3 ± 2.6
	τ_{23} (MPa)	67.0
	τ_{sb} (MPa)	67.7 ± 3.7

Micrographs of the cross sections of the spiral sample, before and after failure in the short beam test, are shown in Fig. 4. The fibers in the E/PU/S sample (Fig. 4a) are aligned at

zero degree and evenly distributed and surrounded by the resin, although there are some imperfections (dark areas). After failure (Fig. 4b), there was a single large transverse fracture at the center of the beam.

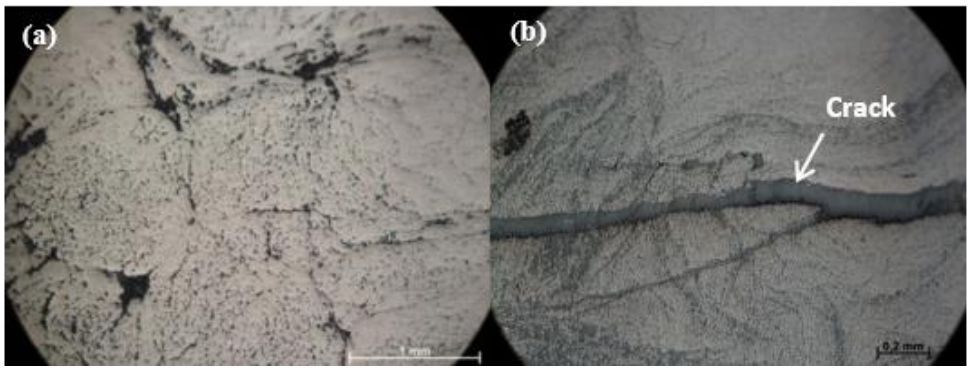

Fig. 4: Cross-section micrographs of the E/PU/S samples before (a) and after (b) failure under short-beam.

4. Modeling

Structural modelling was carried out via Finite Element Method (FEM) using commercial software Abaqus™. The Autodesk Simulation Composite Analysis 2015 plugin was used to evaluate damage/failure process via MCT. Identification of parameters for the elastomeric material was based on the experimental stress vs. strain curve [8], which was interpolated using hyperelastic Arruda-Boyce's model. For the polyester cords, experimental stress vs. strain curve was also obtained [9] and interpolated using the hyperelastic Marlow's model. The steel of the original spiral was simulated by an elasto-plastic model with isotropic hardening, based on typical mechanical properties [10].

Fig. 5 shows details of the FE model. Regarding the boundary conditions, the hose section was fixed in the lower support using a reference point (RP). In the upper support (rigid plate), using another reference point (RP), displacements and rotations were fixed in all directions except the 2-direction (y-direction), where a displacement of 150 mm was gradually applied. Moreover, due to crushing, the outer surface of the hose section can contact the lower and upper supports. Hence, a hard contact was used to simulate the normal interactions and a penalty method was used to simulate the tangential interactions, assuming a coefficient of friction of 0.7 between supports and hose. Embedded elements technique [11] was used to represent that the reinforcement plies and spiral are embedded in the elastomeric body. The reinforcement parts (plies and spiral) and matrix (elastomeric body) are geometrically modelled, separately meshed, and assembled together with embedded elements constraint that relates the degrees of freedom (DOF) of reinforcement to the DOF of the matrix, based on geometric relationships between the nodes of the embedded and the host elements.

The model with steel spiral was meshed using 3D-solid elements. For the elastomeric part, 4800 quadratic hexahedral elements with 20 nodes each one (C3D20) were used. For the reinforcement plies, 35825 linear elements with 4 nodes each one (SFM3D4) were used. Lower and upper supports were defined as rigid surfaces. Mesh-refinement tests were performed considering different numbers of hexahedral and tetrahedral elements for the steel spiral. The crushing load was calculated as a function of the maximum stress in the steel spiral, using the von Mises failure criteria. In all cases, maximum stress was located in the

upper and lower region, near the plates and failure is caused by maximum moment in this region. It is important to highlight that 2D-shell elements were not used in hose section model due to high radius-to-thickness ratio, and it would not be possible to obtain 3D stress state in the spiral.

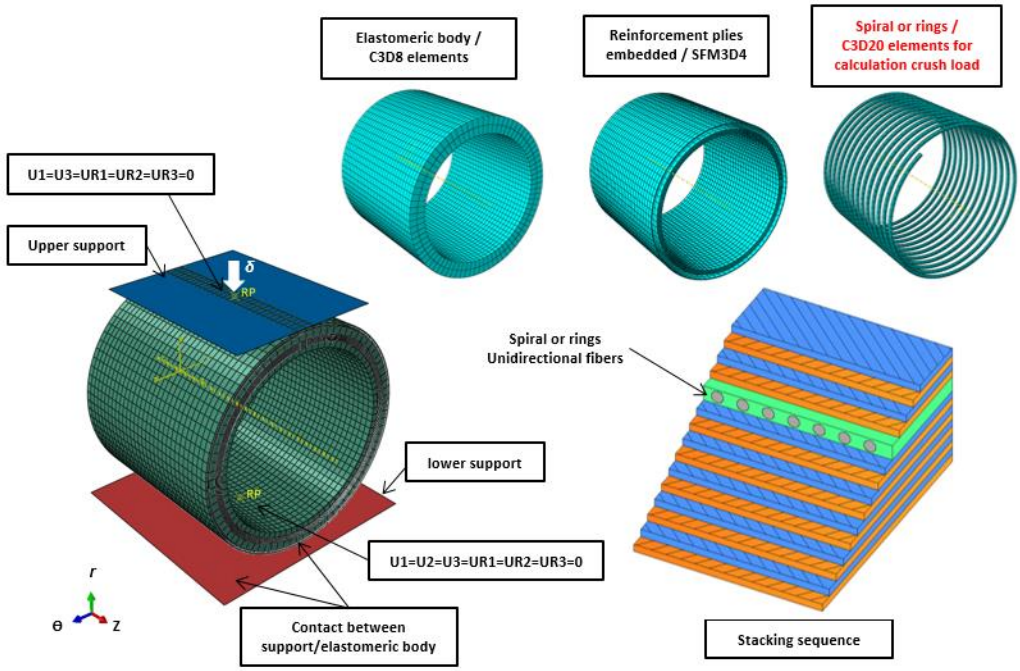

Fig. 5: 3D image and representation of the finite element model used to simulate the hose section under crushing load.

The number of elements varied in each studied configuration as shown in Table 2. For the composite parts, C3D20 elements were used with Hashin criterion for onset failure and MCT approach for damage evolution. It was assumed matrix degradation (E_m^*) of 0.1% for matrix failure, and fiber degradation (E_f*) of 0.001% for fiber failure, based on experimental data provided by Knops and Bögle [12] and simulation results carried out by Nelson et al. [13].

Table 2: Load-bearing components: number of nodes and finite elements.

Nomenclature	***Configuration***	***Cross section***	***Dimensions (mm)***	***Elements***	***Nodes***
ST/S	*Steel spiral*	Circular	Ø=12.7	8750	14016
E/PU/S	*Composite spiral*	Circular	Ø=12.7	46440	264749

5. Crush tests results

Fig. 6 shows the compressive load vs. permanent deflection (inelastic strain) results for experimental crush tests of steel and composite load-bearing components. There are great differences in maximum permanent diameter variation for steel and composite load-bearing components. Permanent deflection after each load increment is low for the composite samples, but is high for the steel spiral (ST/S) even for low loads.

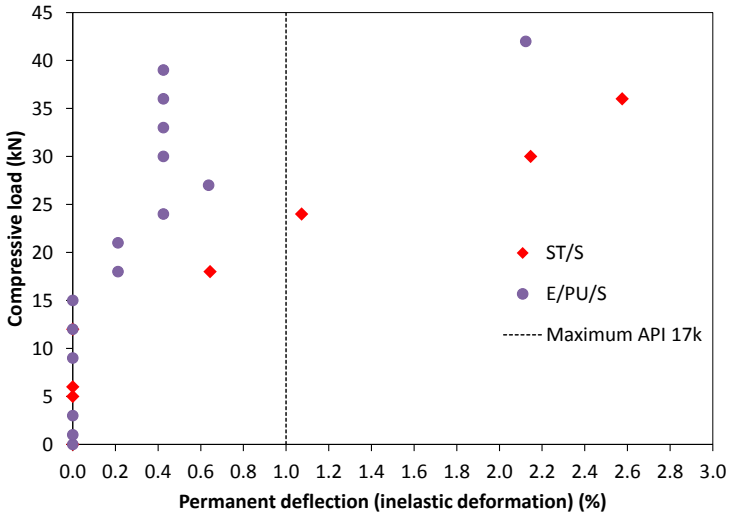

Fig. 6: Compressive load vs permanent deflection (inelastic deformation) results for the various samples.

The ST/S exhibits significant diameter variation (greater than 1%) above 24 kN. However, for the E/PU/S spiral, this was reached only from about 42.0 kN. Moreover, the composite component exhibit permanent deflection only when rupture occurs, but steel samples showed permanent deflection even at low compressive loads. Based on experimental observations, one sample (ST/S) reached maximum permanent diameter variation of 1% and was considered to fail, the composite samples failed because it reached the rupture load, which was 42.0 kN for E/PU/S with a corresponding maximum diameter variation of 2.1%.

The compressive load vs displacement results using the steel spirals ST/S load-bearing component are shown in Fig. 7. The resulting curve of the numerical analysis displays an initial linear behavior. However, for loads greater than 20 kN, non-linear behavior was observed, indicating that the yield stress of 450 MPa was reached. Because of this elasto-plastic behavior, experimental and numerical simulations were completed and it was not evidenced break of the steel spiral.

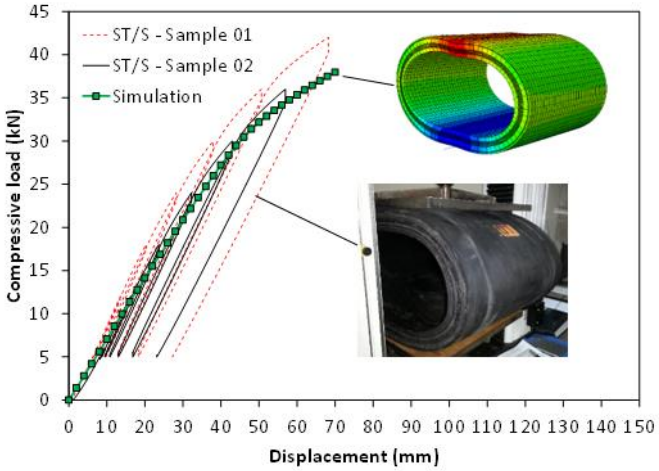

Fig. 7: Compressive load vs displacement curve (numerical and experimental data) for the hose with the steel spiral (ST/S).

6. Progressive Failure Analysis

Fig. 8 shows the numerical and experimental results for the crushing of the hoses with the composite component. For the E/PU/S sample, good correlation between experimental and numerical curves is seen. The numerical maximum load is very similar to the experimental one (around 0.5% deviation), with an associated difference in displacement (around 0.8%). By using the damage model evolution, it was possible to verify that damage was more severe. The greater stiffness of the composite produced with curved pultrusion can lead to more severe localized damage in the part because the applied load is not distributed to the surroundings. Therefore, the composite part fails first, and damage evolution is located in the composite part.

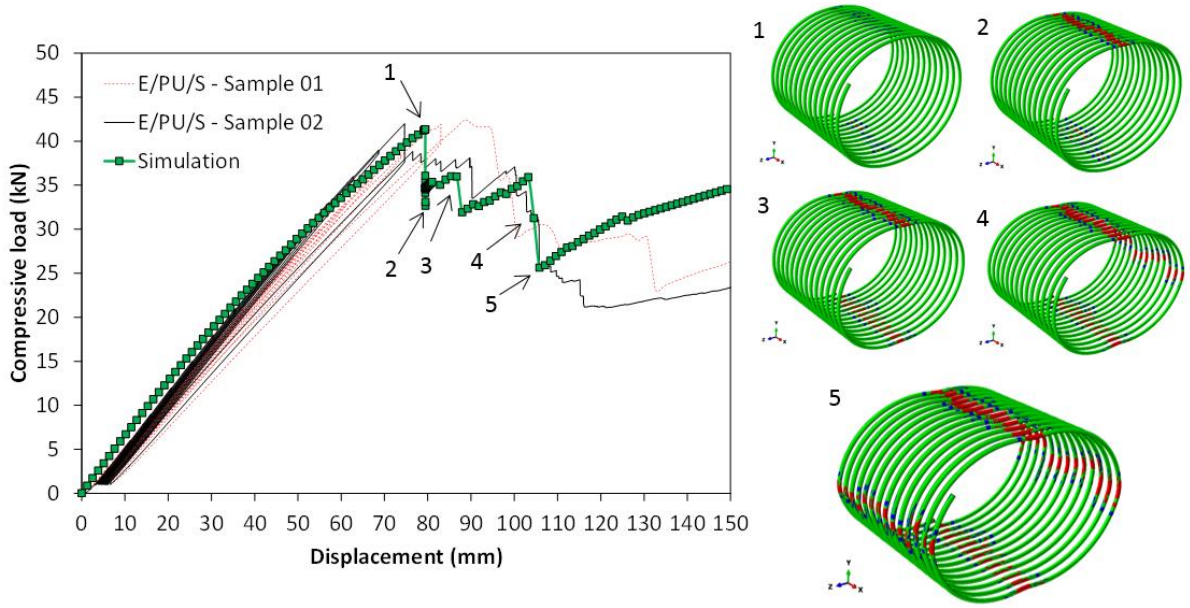

Fig. 8: Compressive load vs displacement curve (numerical and experimental data) for the hose with E/PU/S spiral.

Well defined load peaks are observed in the numerical curves for the hose section. This is caused by failure of the spirals, which occurs in the four regions of stress concentration shown in red in Fig. 8. The first peak in the curve corresponds to failure in the upper region of the spiral and the second failure in the lower region in a very similar load level of the first one. The third failure occurs when one of the lateral regions fails, which is immediately followed by failure of the remaining lateral.

To identify the failure modes, the stress field (σ_{11}, σ_{22}, σ_{33}, σ_{12}, σ_{13}, σ_{23}) predicted by the FE model was investigated. For instance, Fig. 9 shows the stress field before complete failure of the E/PU/S sample. Stress concentrations are observed in the same regions. Comparing the stresses in all directions for the spiral, compressive σ_{11} showed the highest contribution towards failure.

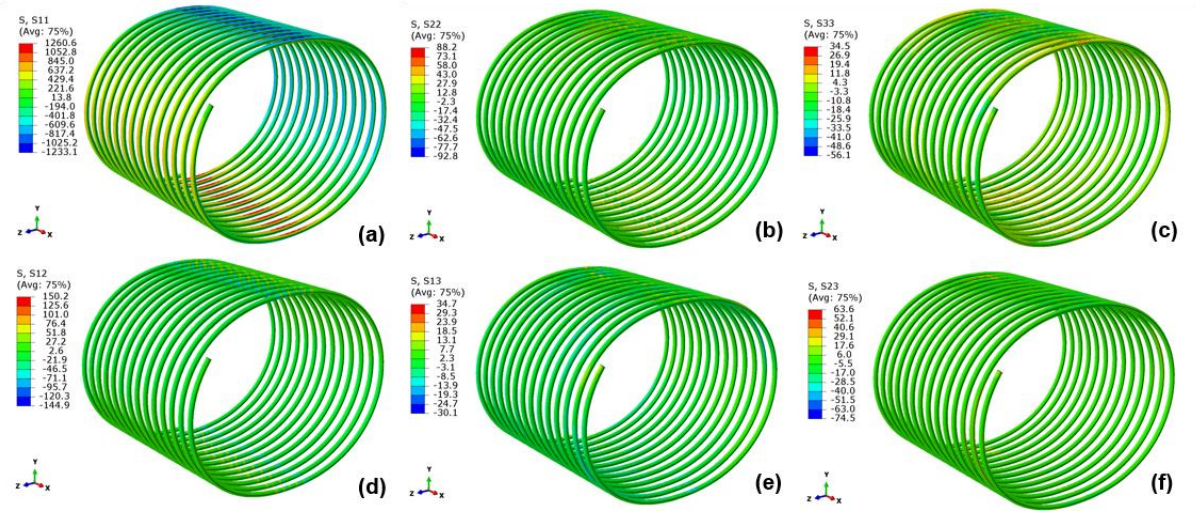

Fig. 9: 3D images of E/PU/S sample under stress just before complete failure: Spiral [σ_{11} (a), σ_{22} (b), σ_{33} (c), σ_{12} (d), σ_{13} (e), σ_{23} (f)].

Fig. 10 shows the displacement field in the E/PU/S sample. Observation of the contact area between the support and the elastomeric part shows good coupling in the model, and the support transfers the load to the entire structure. Moreover, it is possible to observe that the reinforcement plies and the spiral are still embedded in the elastomeric part, as it was found in the actual testing of the hose sections.

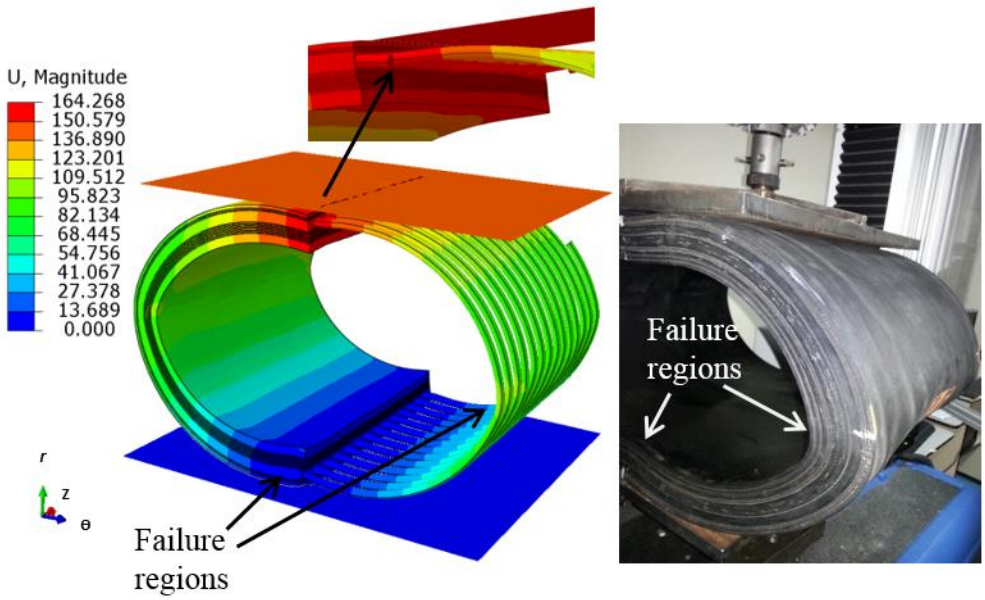

Fig. 10: 3D images showing the displacement field in the y direction and the contact region between support and the elastomeric part with the embedded elements.

7. Conclusions

This study focused on the assessment of the load-bearing components made of composite materials (carbon fiber/epoxy) for an oil offloading hose. A curved composite material was analyzed using a finite element progressive damage model based on Multi-

Continuum Theory (MCT) to predict crushing strength of the central section of the hose with two distinct load-bearing component, one in composite and other in steel. Hyperelastic models were included in the model to predict the rubber and polymeric cords behavior.

The pultruded carbon fiber/epoxy spiral was found to fail due to compressive stress in the fiber, and crushing strength was correctly predicted. The model was highly refined and showed good accordance with the experimental results, where the maximum difference is equal to 2.3% for rupture load of the spiral under fiber-dominated failure. The experimental results and the numerical analysis based on advanced failure criteria and damage evolution have demonstrated that the spiral manufactured by curved pultrusion has great potential to be used as a load-bearing component for offloading hoses, replacing the steel spiral. The manufacture process has influenced in composite strength. The areas rich in resin with randomly distribution improve the strength for the component subjected to bending load.

ACKNOWLEDGEMENTS

The authors gratefully acknowledge Petrobras for the financial support.

REFERENCE

[1] OCIMF 2009. Guide to Manufacturing and Purchasing Hoses for Offshore Moorings. Oil Companies International Marine Forum, London, 2009.

[2] Antal S, Nagy T, Boros A. ARK. Improvement of bonded flexible pipes acc. to new API Standard 17K. In: Offshore Technology Conference; 2003, Houston, May 5-8, p. 8.

[3] Zandiyeh ARK. Fatigue-life prediction in offshore marine hoses. In: Oilfield Engineering with Polymers; 2006, London, March 29-30, p. 12, paper 22.

[4] Lassen T; Lem AI, Imingen G. Load response and finite element modelling of bonded offshore loading hoses. In: Proceedings of the International Conference on Offshore Mechanics and Arctic Engineering - OMAE, 2014, San Francisco, June 8-13, p. 1-17, Paper 23545.

[5] API 17K. Specification for Bonded Flexible Pipe. American Petroleum Institute, Washington, 2006.

[6] Gibson RF. Principles of Composite Material Mechanics. 3rh ed. New York: CRC Press; 2011.

[7] Almeida Jr JHS, Angrizani CC, Botelho EC, Amico SC. Effect of fiber orientation on the shear behavior of glass fiber/epoxy composites. Mater Design 2015; 65: 789–795.

[8] Tonatto MLP, Forte MMC, Araújo RT, Amico SC. Análise numérica da pressão de ruptura de um mangote offloading de dupla carcaça com cordonéis poliméricos. In: 7º Congresso brasileiro de pesquisa e desenvolvimento em petróleo e gás, 2013, Aracaju, October 27-30.

[9] Tonatto MLP, Forte MMC, Roese PB, Araújo RT, Amico SC. Análise numérica da pressão de ruptura de tubos à base de borracha e cordonéis poliméricos, Polímeros 2015; 25: 109-116.

[10] Cabezas EE, Celentano DJ. Experimental and numerical analysis of the tensile test using sheet specimens. Finite Elem Anal Des 2002; 40: 555–575

[11] Abaqus Analysis User's Manual, Version 6.13; 2014.

[12] Knops M, Bogle C. Gradual failure in fibre/polymer laminates. Compos Sci Technol 2006, 66: 616–625.

[13] Nelson E, Hansen AC, Kenik DJ, Tay T. Delamination and damage progression in a composite laminate subjected to bending using multicontinuum theory. In: Structures, Structural Dynamics and Materials Conference AIAA, 2011, Colorado, April 4-7, p. 13.